ELSEVIER

Thin Solid Films 302 (1997) 169–178

thin solid films

Room temperature wafer surface cleaning by in-situ ECR (electron cyclotron resonance) hydrogen plasma for silicon homoepitaxial growth

Hyoun-woo Kim *, Zhen-Hong Zhou, Rafael Reif

Microsystems Technology Laboratory, Massachusetts Institute of Technology, Cambridge, MA 02139, USA

Received 10 October 1996; accepted 15 November 1996

Abstract

A defect-free silicon epitaxial layer was deposited by in-situ electron cyclotron resonance (ECR) hydrogen plasma cleaning at room temperature (25 °C) in a multi-chamber chemical vapor deposition (MS-CVD) system with a load lock chamber. ECR hydrogen plasma was used and films were deposited thermally at low temperature (600 °C). Plain-view transmission electron microscopy (TEM), cross-sectional TEM, Rutherford backscattering spectroscopy, secondary ion mass spectrometry and in-situ emission-Fourier transform infrared spectroscopy results were presented to demonstrate the efficiency of room-temperature in-situ wafer cleaning processes. Process variables such as microwave power (and gas pressure), cleaning temperature and d.c. bias were investigated, and a d.c. bias turned out to play a crucial role in low-temperature in-situ cleaning processes. Also, the effect of the in-situ cleaning temperature on cleaning efficiency was investigated and discussed. The results were shown to help understand the mechanism of the low-temperature wafer cleaning process.

Keywords: Chemical vapour deposition; Hydrogen; Plasma processing and deposition; Transmission electron microscopy

1. Introduction

Lower temperature processing for the semiconductor device fabrication process has been a major issue in solid-state microelectronics and is becoming more important in modern ultra large scale integration technologies. The reduction in temperature may suppress the dopant diffusion so that abrupt transition regions can be obtained. It is crucial to minimize the thermal heating during in-situ cleaning to reduce autodoping and broadening of dopant profile. A low-temperature cleaning technique not only reduces thermal heating during the cleaning process, but it also may be able to lower the subsequent deposition temperature by effectively cleaning the silicon wafer surface before depositing the epitaxial layer.

For low-temperature in-situ cleaning, numerous methods such as Ar ion sputtering [1], Ar/hydrogen ion sputtering [2], and hydrogen plasma cleaning [3] have been tried and investigated. Ar or Ar/H_2 plasma sputtering is an effective cleaning technique but high temperatures were required to anneal out substrate damage which was generated during plasma exposure. The substrate damage is reported to be generated mostly by heavy ion (Ar) bombardment. Compared to conventional r.f. plasma systems, the electron cyclotron resonance (ECR) plasma system can deliver a higher density of low energy ions to the substrate without sacrificing cleaning efficiency. This system is easily and more accurately controlled and substrate damage can be reduced [4]. In-situ wafer cleaning was performed with Ar ECR hydrogen plasma at 600 °C in our system. Epitaxial layers could not be deposited due to the excessive damage on the substrate surface. Therefore it is surmised that the ECR technique may reduce the ion energy. However, once damage was introduced to the substrate, it could not be annealed at temperatures of 600 °C or below.

Hydrogen is the lightest element and is reported to react chemically with carbon or oxygen, so severe substrate damage during ion bombardment may be reduced, while keeping the substrate surface clean. Hydrogen plasma exposure may be based on the ion etching effect [5,6] and the hydrogen passivation effect at low temperatures [7]. Internal reflection measurements showed the presence of Si–H bonds on the HF-treated silicon surface at about a monolayer density [8,9]. H_2 prebake is a simple and reliable

* Corresponding author. 110-304, Banpo Apt., Banpo-Dong, Seo-Cho Gu, 137-040 Seoul, South Korea.

0040-6090/97/$17.00
PII S0040-6090(96)09548-X

method for removing contaminants like carbon and oxygen from the silicon surface [10] but a very high temperature, more than 1000 °C, is required. In an attempt to lower down the prebake temperature, hydrogen plasma exposure has been tried [4].

Although it is required to lower the in-situ cleaning temperature for thermal budget and for future application, the effect of temperature on the in-situ cleaning efficiency has been unclear. Kishimoto et al. [11] studied the temperature dependence of the hydrogen plasma cleaning process by in-situ RHEED monitoring of the cleaned surface. They concluded that the cleaning efficiency was inversely proportional to the cleaning temperature. In our experiments, the temperature dependence of cleaning efficiency was studied by depositing epitaxial layers on the in-situ cleaned surfaces and by observing the structural qualities of those films. Kishimoto et al. suggested a silicon etching mechanism for the in-situ ECR hydrogen plasma cleaning in a temperature range of 300–500 °C. Zhou et al. investigated the mechanisms of room temperature in-situ cleaning with hybrid microwave–r.f. plasma hydrogen plasma by the attenuated total reflection Fourier transform infrared spectroscopy (ATR-FTIR) method [12]. Possible mechanisms need to be investigated and discussed.

2. Experimental

Substrates were 4 inch, czochralski-grown, $< 100 >$-oriented, lightly-doped silicon with 0.5–20 Ω cm resistivity. The wafers were RCA cleaned in an RCA station. A wafer was dipped in 10:1 DI (Deionized) water:HF solution for 20–30 s and then rinsed in deionized water and dried by blowing nitrogen, which was done in an acid-hood in the TRL (Technology Research Laboratory) class 100 cleanroom. After these ex-situ cleaning processes, the wafer was loaded into the load lock chamber of our CVD system.

A multichamber single-wafer chemical vapor deposition reactor was used in our experiments and was located in the TRL cleanroom. After a wafer was loaded into the load lock chamber [13], the load lock chamber was pumped down to about 1×10^{-7} Torr and the wafer was transferred to the analysis chamber by opening the gate valve between the analysis and the load lock chamber. It was then transferred linearly to the CVD chamber, where it was unloaded to the heater stage. After the wafers were loaded onto the heater stage, the base pressure was measured to be around $(1-2) \times 10^{-8}$ Torr.

In-situ predeposition wafer cleaning was done by using ECR hydrogen plasma at room temperature. The hydrogen pressure was kept at 1 mTorr and the flow rate was kept at 20 sccm (standard cubic centimeters per minute) and the in-situ cleaning was carried out for 5 min. ECR was operated at the 2.45 GHz S-band microwave frequency. The window magnet was centered on the top flange of the ECR chamber and the bottom magnet was centered on the lower flange. Their currents were set to 150 A and 120 A, respectively. Deposition was performed by flowing 10 sccm SiH_4 without carrier gases, immediately after the plasma was extinguished. The wafer was then heated up to 600 °C in hydrogen flow with a pressure of 1 mTorr (or 8 mTorr) and a flow rate of 20 sccm. It took about 7 min to heat up from 25 °C to 600 °C, which was a well-characterized deposition temperature in our system. When the in-situ cleaning was done at 250 °C, it took about 4.5 min to heat it up. When the in-situ cleaning was done at 600 °C, the loaded wafer was heated up to 600 °C and then in-situ cleaning was performed. A heater stage was installed to the side of the CVD chamber and the wafer was seated vertically in front of a resistive/radiant heater, which was made of SiC (silicon carbide)-coated graphite.

Rutherford backscattering spectroscopy (RBS) was used to measure the crystalline quality of the epitaxial films. The crystalline quality of the epitaxial film was determined by the ratio of the channeling yield of the film to the random yield (χ_{min}). Cross-sectional transmission electron microscopy (XTEM) was used to observe the epitaxial layer and the epilayer/substrate interface. Plain-view transmission electron microscopy (PTEM) was used to check the epitaxial quality and crystal direction of the deposited films. The TEM used was the model of JEOL 200CX with a LaB_6 filament and line-to-line resolution of about 2.7 Å. The SIMS measurement was done in Evans East, NJ and Cs^+ ion was used as the ion source for sputtering. Carbon and oxygen were detected. Epitaxial film thickness was measured in-situ by the emission Fourier transform infrared spectroscopy (E/FTIR) technique. A Bio-Rad FTIR (model FTS-40) spectrometer equipped with a room temperature deuterated triglycine sulfate (DTGS) detector, was used to collect the emission FTIR spectra. The E/FTIR technique took advantage of the heated wafer as the source of IR radiation. The principles of operation for the E/FTIR were reported elsewhere in detail [14]. A non-contact, non-destructive, real-time, and in-situ epi-film thickness monitoring tool was demonstrated to be useful for observing real time growth rates and an incubation time.

3. Results

Fig. 1(a), 1(b), 1(c), and 1(d) show the XTEM micrographs of Samples A, B, C, and D. All these samples were cleaned in-situ at room temperature. In-situ cleaning conditions for Samples A, B, C, and D are listed in Table 1. In Samples A and B, in addition to having high densities of dislocations and stacking faults, polycrystalline structures were observed (Fig. 1(a) and 1(b)). The bright/dark contrast area just beneath the epilayer/substrate interface in both XTEM micrographs and was interpreted to be damaged regions of a substrate. Their χ_{min} values, which were based on RBS ion channeling experiments, were 27% and

10%, respectively. Samples C and D (Fig. 1(c) and 1(d)) showed defect-free epitaxial layers and continuous interfaces. Their χ_{min} values were measured in the 3–5% range, which confirmed that a good epitaxial film had been deposited. The interface thickness of Sample C was measured to be 20–30 Å and that of Sample D, 30–50 Å.

Fig. 2(a) is the plain-view TEM micrograph, and Fig. 2(b) is the electron diffraction pattern of Sample D. Fig.

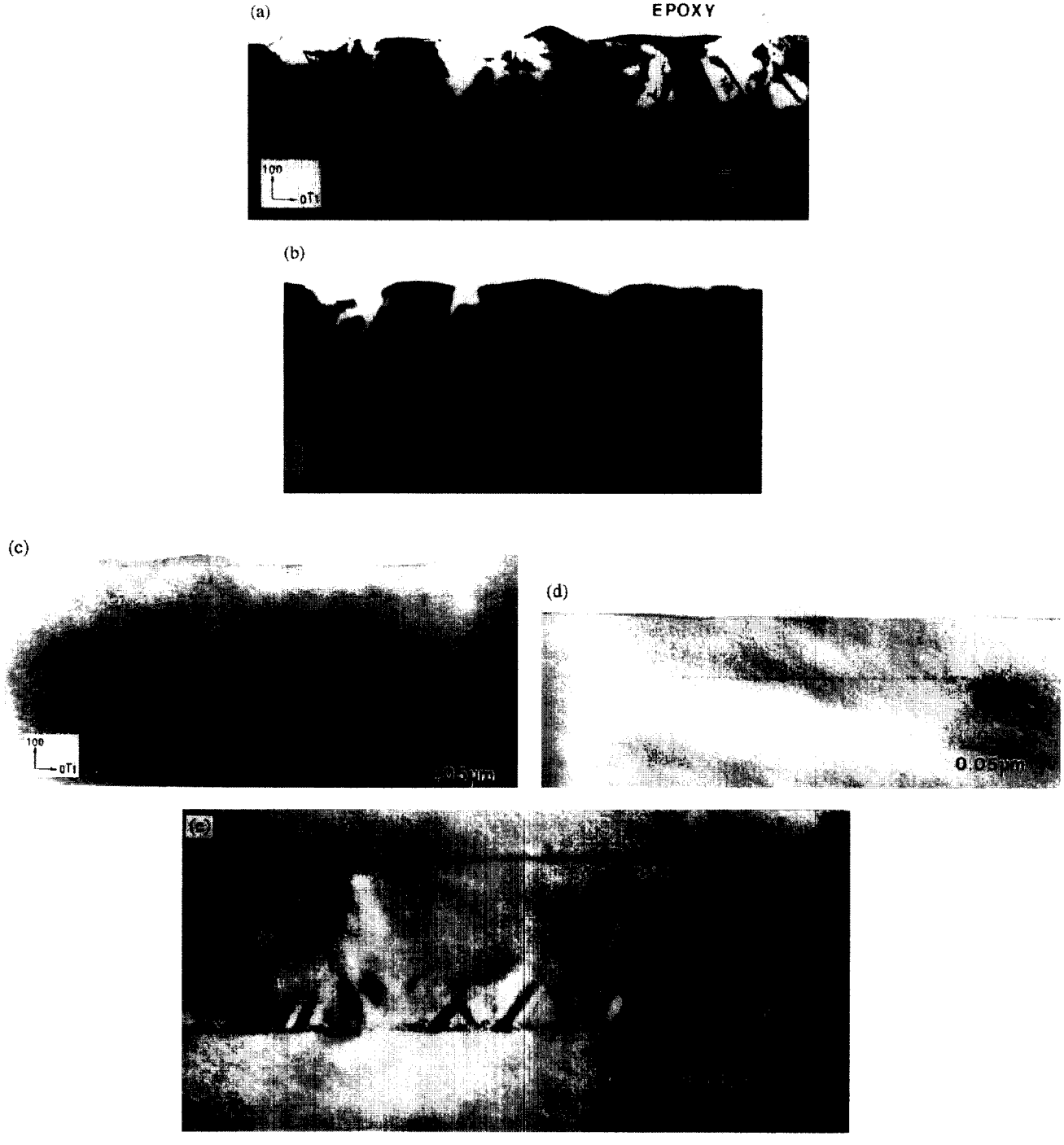

Fig. 1. (a) XTEM micrograph of a polycrystalline film cleaned in-situ at room temperature, with microwave power set at 750 W and d.c. bias set at 0 V. (b) XTEM micrograph of a polycrystalline film cleaned in-situ at room temperature, with microwave power set at 300 W and d.c. bias set at 0 V. (c) XTEM micrograph of an epitaxial film cleaned in-situ at room temperature, with microwave power set at 750 W and d.c. bias set at 10 V. (d) XTEM micrograph of an epitaxial film cleaned in-situ at room temperature, with microwave power set at 300 W and d.c. bias set at 10 V. (e) XTEM micrograph of an epitaxial film cleaned in-situ at room temperature, with microwave power set at 300 W and d.c. bias set at 20 V.

2(a) shows a successfully grown epitaxial layer. Fig. 2(b) corresponds to the electron diffraction pattern of a typical {100} diamond cubic (silicon) structure, which is the same as the diffraction pattern of a {100} substrate. Some extra spots in Fig. 2(b) may represent some contaminants that exist on the outer surface. These contaminants may have come from the atmosphere or they may have been generated during sample preparation. Fig. 3(a) and 3(b) is the real-time in-situ monitoring results of Sample C and Sample A, respectively. Fig. 3(a) does not show an incubation time and shows a well-grown epitaxial layer. Fig. 3(b) shows an incubation time of about 30 min, probably resulting from a deposition on a native oxide which exists on the silicon surface. This E-FTIR technique is suitable for real-time process monitoring and allows an accurate measurement (50 Å resolution) of film thickness. This technique was proven to be useful for studies of incubation time.

Samples C and D received an in-situ cleaning at room temperature with a positive 10 V of d.c. bias. Samples A and B received a room temperature in-situ cleaning with 0 V of d.c. bias. During the application of a 0 V of d.c. bias, a hydrogen ion, accelerated in the sheath region, damaged the substrate and a polycrystalline film was deposited. In other experiments, when hydrogen ion energy was reduced by application of a positive 10 V of d.c. bias, no damage was observed in the epitaxial layer. Probably at low temperatures, the surface damage induced by the hydrogen ion bombardment did not anneal easily. The damage was observed by XTEM analysis. Also from the SIMS and FTIR analysis, oxygen contamination was reduced by application of a positive 10 V of d.c. bias. This may be another reason why defect-free epitaxial layers were deposited.

Fig. 1(e) shows the XTEM micrograph of Sample K. In this experiment, the microwave power was set at 300 W and the d.c. bias was set at a positive 20 V during the room temperature in-situ cleaning. Considerable amounts of stacking faults were generated in the epilayer/substrate interface, and the interface looked broad and contaminated. The thickness was measured to be about 50 Å. This matches our observation: When the in-situ cleaning occurred at 600 °C [15] with a d.c. bias set to a positive 30 V, XTEM analysis revealed that considerable amounts of dislocations and stacking faults were at the epilayer/substrate interface. A large positive d.c. bias reduced the hydrogen ion energy significantly, and surface contaminants, mainly oxygen species, seemed less likely to be removed from the wafer surface under those conditions. From the above experiments, we observed that d.c. bias played a major role in obtaining a defect-free epitaxial layer in the in-situ cleaning process at room temperature.

Table 1
In-situ cleaning conditions (microwave power, d.c. bias, cleaning temperature)

	Microwave power (W)	D.c. bias (V)	Cleaning temperature (°C)
Sample A	750 W (8 mTorr)	0	room T
Sample B	300 W (1 mTorr)	0	room T
Sample C	750 W (8 mTorr)	10	room T
Sample D	300 W (1 mTorr)	10	room T
Sample E	750 W (8 mTorr)	0	600
Sample F	300 W (1 mTorr)	0	600
Sample G	750 W (8 mTorr)	10	600
Sample H	300 W (1 mTorr)	10	600
Sample I	300 W (1 mTorr)	10	280
Sample J	300 W (1 mTorr)	10	480
Sample K	300 W (1 mTorr)	20	room T

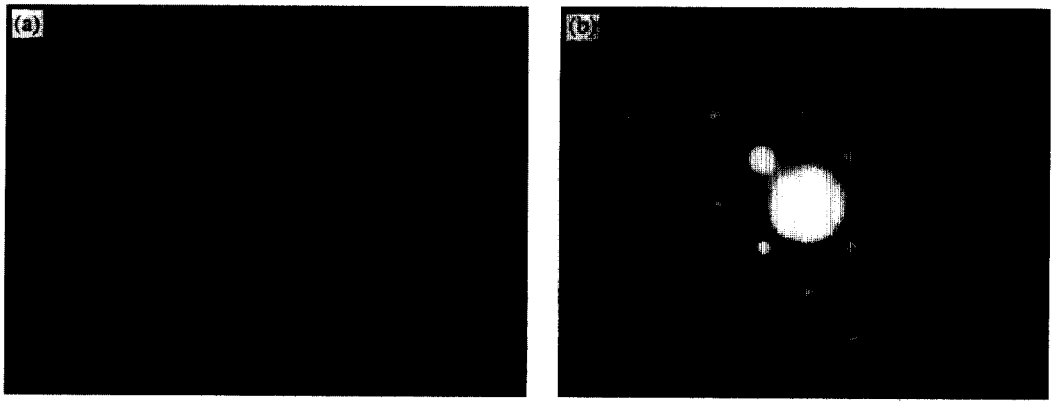

Fig. 2. (a) Plain-view TEM micrograph of an epitaxial film cleaned in-situ at room temperature, with microwave power set at 300 W and d.c. bias set at 10 V. (b) Electron diffraction pattern of an epitaxial film cleaned in-situ at room temperature, with microwave power set at 300 W and d.c. bias set at 10 V.

Table 2
SIMS and RBS data

	Oxygen (cm^{-2})	Oxygen (cm^{-3})	Carbon (cm^{-2})	Carbon (cm^{-3})	χ_{min}
Sample A^+	1.0×10^{15}	7×10^{20}	1.1×10^{14}	1×10^{20}	7%
Sample A	1.1×10^{15}	3×10^{20}	1.5×10^{13}	9×10^{18}	27%
Sample B	8.5×10^{14}	1×10^{21}	8.0×10^{12}	7×10^{18}	10%
Sample C	3.0×10^{14}	3×10^{20}	6.9×10^{12}	6×10^{18}	3–5%
Sample D	7.8×10^{14}	7×10^{20}	1.4×10^{13}	1×10^{19}	5%
Sample E	9.7×10^{14}	9×10^{20}	2.6×10^{13}	2×10^{19}	5%
Sample F	8.1×10^{14}	3×10^{20}	3.8×10^{13}	3×10^{19}	5%
Sample G	4.9×10^{14}	3×10^{20}	2.6×10^{13}	2×10^{19}	3–5%
Sample H	4.8×10^{13}	8×10^{19}	4.5×10^{14}	5×10^{20}	3%

Sample A^+ received the same ex-situ cleaning but no in-situ cleaning was performed before the epitaxial deposition. Stacking faults were initiated in the epilayer/substrate interface. By SIMS analysis (Table 2), the interfacial oxygen concentration (areal density) was 1.0×10^{15} atoms cm^{-2} and the oxygen species in the interface may have been on the initial silicon surface before loading into the chamber. Native oxides may have grown during the water rinsing process. By comparing Samples D or C with Sample A^+ in their XTEM micrographs, the room-temperature cleaning with an appropriate positive d.c. bias was effective in removing contaminants which came from the ex-situ wafer cleaning.

Four pairs of samples (Samples A and E, Samples B and F, Samples D and H, and Samples C and G) were compared: the room temperature in-situ cleaning vs. the high temperature (600 °C) in-situ cleaning. Table 1 shows the in-situ cleaning conditions (microwave power (gas pressure), d.c. bias, cleaning temperature) of each sample. Microwave power (gas pressure) was set at 750 W (8 mTorr) and 300 W (1 mTorr), d.c. bias was set at 0 V and 10 V. Cleaning temperature was set at room temperature and at 600 °C.

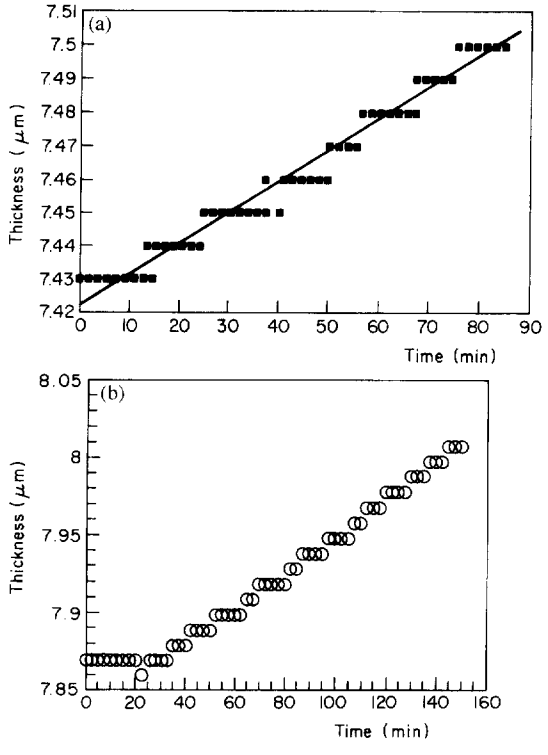

Fig. 3. (a) Real-time in-situ monitoring of film thickness for a defect-free epitaxial film. (b) Real-time in-situ monitoring of film thickness for a polycrystalline film.

Fig. 4(a) and 4(b) are the XTEM micrographs of Samples E and F, respectively. Samples E and F received a high-temperature (600°C) in-situ cleaning. Samples A and E were compared. In Fig. 4(a) Sample E showed an epitaxial layer although there were some defects near the interface. Samples B and F were compared. Fig. 4(b) shows that Sample F had an almost defect-free epitaxial layer with a continuous epilayer/substrate interface. Sample H was compared with Sample D: both samples show defect-free epitaxial layers, although Sample H has an almost invisible interface, as was shown in the high-resolution cross-sectional transmission electron microscopy (HRXTEM) micrograph [16]. Samples G and C were compared. Sample G shows an epitaxial layer, however, its interface has some stacking faults and other defects. In both samples, their χ_{min}'s were in the 3–5% range. In our structural analysis, room temperature in-situ cleaning was found to be an efficient cleaning process and comparable to the higher temperature cleaning processes at 600 °C. Efficient cleaning could be achieved by choosing an appropriate d.c. bias.

By using column bar graphs, a more systematic analysis on the eight samples (Samples A, B, C, D, E, F, G, and H) will help verify the above findings and help understand the room temperature in-situ cleaning process. The χ_{min} values of epitaxial layers were measured by RBS analysis.

Table 3
Experimental conditions for categories of Fig. 5(a)

	Microwave power (W)	Pressure (mTorr)	D.c. bias (V)
1	750	8	0
2	300	1	0
3	750	8	10
4	300	1	10

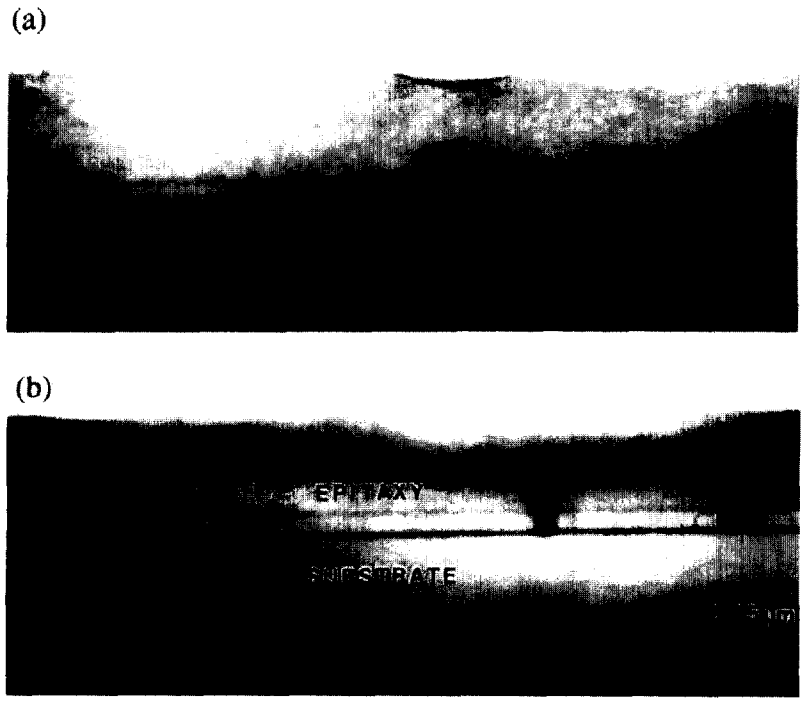

Fig. 4. (a) XTEM micrograph of an epitaxial film cleaned in-situ at 600 °C, with microwave power set at 750 W and d.c. bias set at 0 V. (b) XTEM micrograph of an epitaxial film cleaned in-situ at 600 °C, with microwave power set at 750 W and d.c. bias set at 10 V.

Interfacial oxygen and carbon concentrations were measured by SIMS. Interfacial impurity concentration was represented by its areal density, instead of volume concentration at a particular interface.

Fig. 5(a) shows the effect of cleaning temperature on the interfacial carbon concentration. Experimental conditions for categories of Fig. 5(a) are shown in Table 3. For every pair of samples, the sample which received the room temperature in-situ cleaning had a lower carbon concentration in its epilayer/substrate interfaces than did the sample

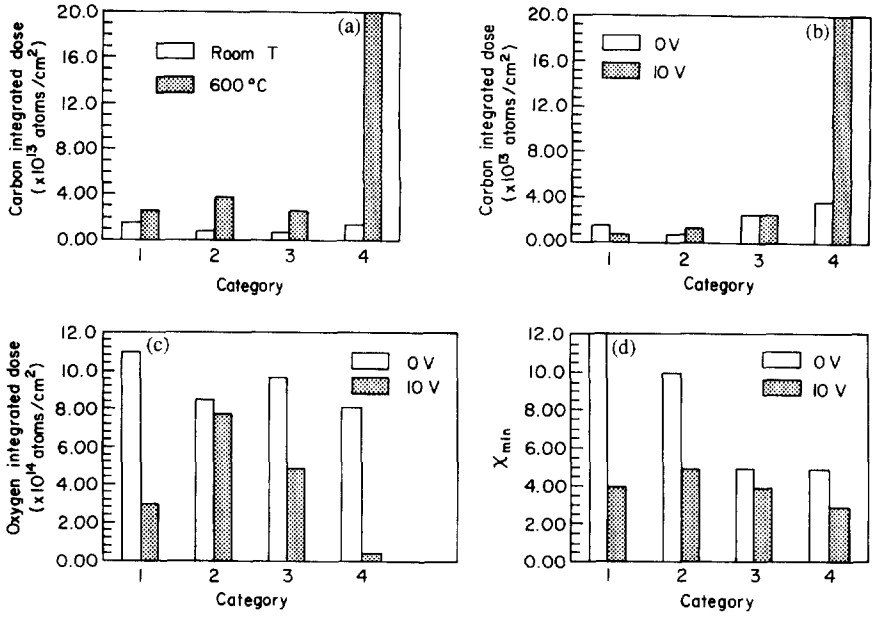

Fig. 5. (a) Column bar graph showing the effect of cleaning temperature on interfacial carbon concentration. (b) Column bar graph showing the effect of substrate d.c. bias on interfacial carbon concentration. (c) Column bar graph showing the effect of substrate d.c. bias on interfacial oxygen concentration. (d) Column bar graph showing the effect of substrate d.c. bias on the χ_{min} value of the film.

Table 4
Experimental conditions for categories of Fig. 5(b)

	Microwave power (W)	Pressure (mTorr)	Temperature (°C)
1	750	8	room T
2	300	1	room T
3	750	8	600
4	300	1	600

which received the in-situ cleaning at 600 °C. Interfacial carbon concentrations of the samples which received the room-temperature in-situ cleaning were even lower than those of Sample A^+. Sample A^+ did not receive an in-situ wafer cleaning after ex-situ wafer cleaning and its interfacial carbon concentration was 1.1×10^{14} atoms/ cm^{-2}. Fig. 5(b) shows the effect of substrate d.c. bias on the interfacial carbon concentration. Experimental conditions for categories of Fig. 5(b), 5(c) and 5(d) are listed in Table 4. A d.c. bias was not an important process variable affecting the interfacial carbon concentration. Therefore, a hydrogen ion does not play a major role in removing carbon from the silicon surface and the carbon removal process will be a hydrogen chemical etching process which corresponds to the interaction of atomic hydrogen with carbon species, such as the methyl group, as an example [17].

The interfacial carbon concentration does not seem to affect the quality of the epitaxial layer and Kim et al.'s studies also support our observation [18]. β-SiC was formed in the interface during epitaxial growth at 1000 °C, the presence of the β-SiC does not affect the crystalline quality of the epitaxial layer. The solubility of carbon in solid silicon is known to be 3.5×10^{17} atoms cm^{-3} or slightly less at the melting point (about 1400 °C) [19]. In our samples, carbon concentration is above 1×10^{18} atoms cm^{-3} at or near the interface, most interface carbons are supposed to precipitate as β-SiC from thermodynamic considerations. However, in order for carbons to precipitate, many carbon atoms must condense and the probability of their encounter is quite small due to their low concentrations. β-SiC formed when chemically prepared silicon surfaces are heated to 800 °C [20] and the carbide was not formed below 700 °C [21,22]. In our case of low temperature processing (≤ 660 °C), it is not clear whether the carbide was formed or not.

Fig. 5(c) shows the effect of a d.c. bias on the interfacial oxygen concentration. The interfacial oxygen concentration of the sample was affected by a substrate d.c. bias. The samples which received an in-situ cleaning with 10 V of d.c. bias had a particularly reduced oxygen concentration when compared to the samples which received an in-situ cleaning with 0 V of d.c. bias. The removal of oxygen species is an ion etching process [15,23], with an impinging hydrogen ion which damages the surface and increases its reactivity. Hydrogen neutrals or ions react with some Si–O bonding configuration and volatile species are desorbed from the surface. In our analysis, the surface oxygen concentration was reduced by adjusting the hydrogen ion energy with a substrate d.c. bias. In room temperature in-situ cleaned samples (first and second categories) oxygen concentrations were not as much affected by a d.c. bias as the 600 °C cleaned samples (third and fourth categories) were. So it may be inferred that 0 V biased in-situ cleaning, which provides higher ion energy than +10 V biased cleaning, degraded the epitaxial quality during room-temperature in-situ cleaning. In this case, hydrogen ions damaged the substrates, not only to activate it but also generated the unwanted defects. This finding matches with the observation made by XTEM analysis.

For most pairs of samples, the sample which received the room-temperature cleaning had the higher χ_{min} value. In other words, its structural quality was inferior to the sample which received the in-situ cleaning at 600 °C. This tendency was more evident in the case of the first two categories, where the d.c. bias was set at 0 V. Fig. 5(d) shows the effect of a d.c. bias on the χ_{min} value of the film. Samples which received an in-situ cleaning with a 0 V of d.c. bias had an inferior structural quality compared to samples which received a cleaning with 10 V of d.c. bias. This tendency was more evident in the first two categories, which are room temperature in-situ cleaned samples. Fig. 5(c) and 5(d) can be compared, interfacial oxygen concentrations are closely related to the crystalline qualities of epitaxial layers. In our analysis, hydrogen gas density (represented by microwave power and gas pressure) did not affect the film quality significantly, in the range from 300 W (1 mTorr) to 750 W (8 mTorr), compared to d.c. bias and cleaning temperature (both high gas pressure and high microwave power correspond to high gas density, and vice versa). This is another evidence that the impurity (oxygen) removal is not a purely chemical process. In this case, high pressure reduce the amounts of ions which strike the wafer surface by high collision in the sheath region, although more ions were produced by applying high microwave power.

Current literature reports that lower temperature in-situ cleaning might be more efficient than higher temperature cleaning in removing oxygen contaminants because at higher temperatures, the sticking coefficient of hydrogen to the silicon surface decreases and hydrogen atoms are easily desorbed and hydrogen passivation will be lost [24]. Oxygen removal is affected by hydrogen passivation. In this case, the sticking coefficient of the hydrogen radicals decreases at higher temperatures and may take longer to clean the surface at the higher temperature. But this observation does not necessarily apply to our system because although in-situ wafer cleaning can be performed at room temperature, the temperature should be raised to at least 600 °C in our depositions for actual epitaxial growth to be initiated. It took at least 7 min to heat the wafer from room temperature to 600 °C in our system and hydrogen passivation may be lost during this process. It was shown by SIMS that some oxygen and carbon may have stuck onto

the silicon surface, when hydrogen was kept flowing at 600 °C. But this oxygen contamination may be reduced at higher temperatures because of oxygen desorption phenomena. It can be assumed that oxygen desorbs at high temperatures. Also, oxygen removal is feasible only for weakly adsorbed oxygen [25], since the surface reaction between reactive species and passivation oxide films proceeds very slowly at temperatures less than 800 °C [26]. Even for submonolayer coverage of oxygen on silicon, the desorption temperature of the oxide, such as SiO, was reported to be about 700 °C [27]. If the oxide layer is sufficiently thick from the beginning, or the cleaning temperature is so low that the desorption process becomes a rate-determining step, the rate of oxygen removal and thus the cleaning efficiency will increase with increasing temperature.

In addition, experiments (using Samples I, J) were performed to investigate the effect of cleaning temperatures between 25 °C and 550 °C, on cleaning efficiency in terms of structural analysis. In-situ cleaning was performed with a microwave power of 300 W and a d.c. bias of +10 V, for both samples. In Sample I, in-situ cleaning was done at 280 °C and the wafer was heated up during hydrogen flowing for about 4.5 min. Deposition was performed at 600 °C. The XTEM micrograph of Sample I shows that an almost defect-free epitaxial layer was deposited. The thickness of epilayer/substrate interface was about 20 Å. The purpose of this experiment was to reduce the hydrogen exposure time and at the same time to lower the cleaning temperature as much as possible.

Fig. 6(a) is the XTEM micrograph of Sample J. In-situ cleaning was carried out at 480 °C. The plasma was turned off after 5 min and silane was introduced immediately at the same temperature. Deposition temperature was adjusted to 600 °C afterwards. Although hydrogen passivation may have begun to be lost at low temperatures at about 400 °C [28], if we accept the report that the hydrogen desorption temperature is between 510 and 520 °C [29], some hydrogen species may stay at 480 °C so that they prevent oxygen species from being adsorbed on the silicon surface. From the micrograph, a defect-free epitaxial layer was grown and the epilayer/substrate interface was thin (less than 20 Å). However, the interface clearly existed and was not invisible. There should be some remaining oxide or surface contaminants, probably due to low initial deposition temperature. Samples D, I, J, and H were compared, to see the effect of the cleaning temperature to the cleaning efficiency. The thickness of epilayer/substrate interface was plotted as a function of cleaning temperature (Fig. 6(b)). Averaged values were used for the interface thicknesses and possible measurement error was considered. The interface thicknesses for Samples D, I, J, and H were in the range of between 10 and 50 Å, and showed a slight decrease as cleaning temperature increased from 25 °C to 600 °C. It is shown that the structural qualities of epitaxial layers are not affected by the in-situ cleaning temperature significantly, as long as standard conditions hold.

(a)

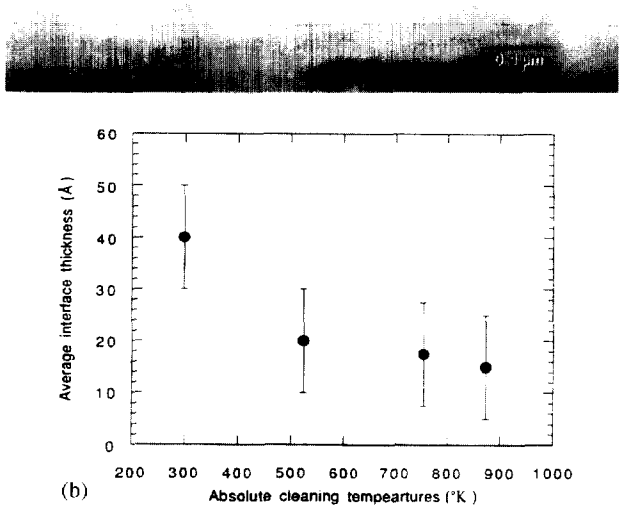

Fig. 6. XTEM micrograph of an epitaxial film, cleaned in-situ with standard conditions at 480 °C. (b) Average thickness of the epilayer/substrate interface as a function of cleaning temperature.

4. Discussion

The mechanism of carbon removal at low temperature ($\leq$ 700 °C) is not clear. Thomas et al. suggested that removal of surface carbon occur by volatilization through hydrogenation in hydrogen plasma cleaning process. Licciardello et al. suggested that after HF dipping, organic compounds are chemically bonded to the silicon surface and this organic layer will not be affected by the growth of surface oxide layer [30]. Kinoski et al. found that removal of carbon at 400 °C was less efficient than at 250 °C in their hydrogen plasma cleaning experiments. It is thought that the carbon removal mechanism was related to the removal of methyl group from the surface by H (g) [25]. Cheng et al. also observed that the carbon removal rate decreased with increasing temperature at temperatures above 177 °C in their experiments on the interaction of atomic hydrogen with surface methyl group on Si(100) [17]. Surface carbon present as CH_3 (ad) was removed by the chemical reaction, producing volatile methylsilane, CH_3SiH_3 (g).

Colaianni et al. investigated the behavior of Si–CH_3 at low temperatures ($\leq$ 577 °C). At above 427°C, CH_3 (ad) has begun to decompose to CH_2 (ad) and/or CH(ad) species and at above 577 °C, only the presence of adsorbed carbon on the surface was verified [31]. Therefore, at temperatures below 327 °C, surface carbon will be present as CH_3 (ad) and this can be removed easily by reactions

Table 5
Free energy changes for oxygen removal reactions with plasma excitement (J mole^{-1}) [34–37]

Possible reactions	25 °C	600 °C
(1) SiO_2 (s) + H (g) → SiH (g) + O_2 (g)	934530	800653
(2) SiO_2 (s) + 2H (g) → SiO (g) + H_2O (g)	32657	-28105
(3) SiO_2 (s) + 2H (g) → SiH_2 (g) + O_2 (g)	592468	419086
(4) SiO_2 (s) + 4H (g) → Si (s) + $2H_2O$ (g)	-475176	-396011
(5) SiO_2 (s) + 4H (g) → SiH_4 (g) + O_2 (g)	38815	112676
(6) SiO_2 (s) + 5H (g) → SiH (g) + $2H_2O$ (g)	-335746	-288993
(7) SiO_2 (s) + 6H (g) → SiH_2 (g) + $2H_2O$ (g)	-677748	-670550
(8) SiO_2 (s) + 8H (g) → SiH_4 (g) + $2H_2O$ (g)	-1231461	-976960

$Si-CH_3 + 3H\ (g) \rightarrow CH_3SiH_3\ (g)$ [17]. In carbon removal process, etchant are formed and these etchant will be adsorbed on the substrate for subsequent reaction. And product should be desorbed, for etching to be continued. In ECR hydrogen plasma, hydrogen gas (H_2(g)) will be converted into more reactive H (g), at low temperatures (< 600 °C) the above reaction will occur and volatile CH_3SiH_3 (g) will be produced. It was shown in Fig. 6.11(b) that a low temperature is favored for carbon removal. Therefore, desorption of reaction products will not be a rate-determining step in carbon removal processes, adsorption/reaction can be a rate-determining step.

In ECR hydrogen plasma, dissociation, direct ionization and dissociative ionization of H_2 (g) will occur in the plasma chamber [26]. Dissociation reaction can be written as: $H_2\ (g) + e^- \rightarrow 2H\ (g) + e^-$. Burke et al. found that in his ECR hydrogen cleaning experiments, atomic hydrogen produced in the plasma was the dominant agent during the cleaning process, in reducing the native oxide and the carbonated compounds [32]. In our system, it was assumed that $SiO_2 + nH\ (g)$ ($n = 1, 2, \ldots$) occurred and their free energy changes are listed in Table 5. Reactions (4), (5), (6), (7), and (8) cannot be dominant reactions because these reactions are thermodynamically more favorable at lower temperature and does not match with our observation. In Reaction (3), $\Delta G_{600\ °C} = 419086$ J and at equilibrium, $P_{SiH2} P_{O2} = 8.4 \times 10^{-34}$ Torr^2 and this reaction cannot occur (it was assumed here that $P_H = 0.1$ mTorr, by considering ionization efficiency of 0.1). In Reaction 1, $\Delta G_{600\ °C} = 800653$ J and at equilibrium, $P_{SiH} P_{O2} = 9.3 \times 10^{-50}$ Torr^2. Reaction (1) will not occur in our system. Therefore, Reaction (2): SiO_2 (s) + 2H (g) → SiO (g) + H_2O (g) will be a dominant reaction. Since $\Delta G_{600\ °C} = -28105$ J and at equilibrium, $P_{SiO} P_{H2O} \cong 2.7 \times 10^{-7}$ Torr^2. If $P_{H2O} = 10^{-8}$ Torr, $P_{SiO(eq)} = 27$ Torr by calculation, this reaction has a high driving force to proceed. Also, $\Delta G_{25\ °C} = 32657$ J and at equilibrium, $P_{SiO} P_{H2O} \cong 1.9 \times 10^{-14}$ Torr^2 and if $P_{SiO} = P_{H2O}$, $P_{SiO} = P_{H2O} \cong 1.4 \times 10^{-7}$ Torr and the reaction will proceed even at room temperature. The oxygen removal process with hydrogen plasma excitation will be reaction controlled or desorption controlled. By Reaction (2), SiO (g) and H_2O (g) are desorbed. The boiling point of SiO (g) is known to be lower than that of H_2O (g); SiO (g) is a volatile product. So it is possible that the removal process is dominated by desorption of water vapor.

Sample A$^+$ was rinsed and blow-dried, then heated up to 600 °C for subsequent epitaxial growth. Its interfacial oxygen concentration was measured to be 1.0×10^{15} atoms cm^{-2}. By comparing Samples H and D, the standard in-situ plasma cleaning at 600 °C and at room temperature may be compared directly. Their SIMS data are shown in Table 2. Both samples were rinsed and blow-dried and heated up to 600 °C for 7 min. By calculation, the room temperature in-situ cleaning reduced $1.0 \times 10^{15} - 7.8 \times 10^{14} = 2.2 \times 10^{14}$ oxygen atoms cm^{-2}. The standard in-situ cleaning at 600 °C reduced $1.0 \times 10^{15} - 4.8 \times 10^{13} = 9.5 \times 10^{14}$ oxygen atoms cm^{-2}. Therefore, in-situ plasma cleaning was more efficient at higher temperature in removing oxygen contaminants in our system. Room temperature in-situ cleaning removed 2.2×10^{14} oxygen atoms cm^{-2} and in-situ cleaning at 600 °C removed 9.5×10^{14} oxygen atoms cm^{-2}. Since the in-situ cleaning was performed for 300 s, oxygen removal rates were 6.7×10^{11} atoms cm^{-2} s at room temperature and 3.2×10^{12} atoms cm^{-2} s at 600 °C. The kinetic expression can be written as: rate $= A \exp(-E/RT)$ and if it is assumed that E is not a function of temperature,

$$\ln \frac{\text{rate at } T_2}{\text{rate at } T_1} = \frac{E}{R}\left(\frac{1}{T_1} - \frac{1}{T_2}\right)$$

By substituting $T_1 = 298$ K and $T_2 = 873$ K and $R = 8.314$ J deg^{-1} mole^{-1}, $E = 5500$ J mole^{-1}. Heat of evaporation of water is 41090 J mole^{-1} at 100 °C [33]. If it is assumed that the activation energy of the desorption process is equal to the heat of evaporation of water vapor, oxygen removal process with plasma excitation is shown to be reaction controlled.

5. Summary

Defect-free epitaxial layers were deposited by applying the room temperature in-situ wafer cleaning processes with a positive 10 V of d.c. bias. Polycrystalline films were deposited by the application of a 0 V of d.c. bias. The cleaning process with a 20 V of d.c. bias was not effective. The samples which received the room temperature in-situ cleaning had a lower interfacial carbon concentration than those of the samples which received the in-situ cleaning at 600 °C and the samples which did not receive the in-situ wafer cleaning. In room-temperature in-situ ECR hydrogen plasma cleaning, the carbon removal process was a hydrogen chemical etching process, while the removal of oxygen species was an ion-etching process. The interfacial carbon concentration was not affected by substrate d.c. bias, while the interfacial oxygen concentration was reduced by adjusting the hydrogen ion energy with a substrate d.c. bias.

Acknowledgements

This work was funded by SEMATECH.

References

[1] R. Reif, *J. Vac. Sci. Technol., A2* (1984) 429.
[2] T.R. Yew, R. Reif, *J. Appl. Phys., 68* (9) (1990) 4681.
[3] I. Suemune, Y. Kunitsugu, Y. Tanaka, Y. Kan and M. Yamanishi, *Appl. Phys. Lett., 53* (1988) 2173.
[4] R.E. Thomas, M.J. Mantini, R.A. Ruddler, D.P. Malta, S.V. Hattangady and R.J. Markunas, *J. Vac. Sci. Technol., A10* (4) (1992) 817.
[5] H.W. Kim and Z.H. Zhou, *Thin Solid Films.*
[6] M. Delfino, S. Salimian, D. Hodul, A. Ellingboe and W. Tsai, *J. Appl. Phys., 71* (2) (1992) 1007.
[7] B.S. Meyerson, *Proc. IEEE, 80* (10) (1992) 1594.
[8] E. Yablonovitch, D.L. Allara, C.C. Chang, T. Gmitter and T.B. Bright, *Phys. Rev. Lett., 57* (1986) 249.
[9] V.A. Burrows, Y.J. Chabal, G.S. Higashi, K. Raghavachari and S.B. Christman, *Appl. Phys. Lett., 53* (1988) 998.
[10] T.Y. Hsieh, K.H. Jung and D.L. Kwong, *J. Electrochem. Soc., 138* (4) (1991) 1188.
[11] A. Kishimoto, I. Suemune, K. Kamaoka, T. Koui, Y. Honda and M. Yamanishi, *Jpn. J. Appl. Phys., 29* (10) (1990) 2273.
[12] Z.H. Zhou, E.S. Aydil, R.A. Gottscho, Y.J. Chabal and R. Reif, *J. Electrochem. Soc., 140* (11) (1993) 3316.
[13] Z.H. Zhou, *M.Sc. Thesis,* 1991, p. 24.
[14] Z.H. Zhou, F.Z. Yu and R. Reif, *J. Vac. Sci. Technol., B9* (2) (1991) 374.
[15] H.W. Kim, *Ph.D. Thesis,* 1994, p. 64.
[16] Z.H. Zhou, H. Kim and R. Reif, *Mater. Res. Soc. Symp. Proc., 324* (19984).
[17] C.C. Cheng, S.R. Lucas, H. Gutleben, W.J. Choyke and J.T. Yates, Jr., *Surf. Sci. Lett., 273* (1992) L441–L448.
[18] K. Kim, P. Maillot, A.E. Morgan, A. Kermani and Y.H. Ku, *J. Appl. Phys., 67* (4) (1990) 2176.
[19] T. Nozaki, Y. Yatsurugi and N. Akiyama, *J. Electrochem. Soc., 117* (12) (1970) 1566.
[20] R.C. Henderson, R.B. Marcus and W.J. Polito, *J. Appl. Phys., 42* (1971) 1208.
[21] R.E. Thomas, M.J. Mantini, R.A. Rudder, D.P. Malta, S.V. Hattangady and R.J. Markunas, *J. Vac. Sci. Technol., A10* (4) (1992) 817.
[22] M.J. Bozack, P.A. Taylor, W.J. Choyke and J.T. Yates, Jr., *Surf. Sci., 177* (1986) L933.
[23] M. Delfino, S. Salimian, D. Hodul, A. Ellingboe and W. Tsai, *J. Appl. Phys., 71* (2) (1992) 1007.
[24] A. Kishimoto, I. Suemune, K. Kamaoka, T. Koui, Y. Honda and M. Yamanishi, *Jpn. J. Appl. Phys., 29* (10) (1990) 2273.
[25] D. Kinoski, R. Qian, A. Lahajan, S. Thomas, P. Munguia, J. Fretwell, S. Banerjee and A. Tasch, *Mater. Res. Soc. Symp. Proc., 315* (1993) 223.
[26] H. Yamada, *J. Appl. Phys., 65* (2) (1989) 776.
[27] J.R. Engstrom, D.J. Bonser, M.M. Nelson and T. Engel, *Surf. Sci., 256* (1991) 317.
[28] S.S. Iyer, M. Arienzo and E. de Fresart, *Appl. Phys. Lett., 57* (9) (1990) 895.
[29] S.H. Wolff, S. Wagner, J.C. Bean, R. Hull and J.M. Gibson, *Appl. Phys. Lett., 55* (19) (1989) 2017.
[30] A. Licciardello, O. Puglisi and S. Pignataro, *Appl. Phys. Lett., 48* (1) (1986) 42.
[31] M.L. Colaianni, P.J. Chen, H. Gutleben and J.T. Yates Jr., *Chem. Phys. Lett., 191* (6) (1992) 561.
[32] R. Burke, J. Pelletier, C. Pomot and L. Vallier, *J. Vac. Sci. Technol., A8* (3) (1990) 2931.
[33] D.R. Gaskel, *Introduction to Metallurgical Thermodynamics,* McGraw-Hill, New York, 1981.
[34] M.D. Allendorf and C.F. Melius, *J. Phys. Chem., 96* (1) (1992) 428.
[35] *JANAF Thermochemical Tables.*
[36] Samsonov, *The Oxide Handbook.*
[37] L. Fredin, R.H. Hauge, Z.H. Kafari and J.L. Margrave, *J. Chem. Phys., 82* (8) (1985) 3544.